FULL PAPER *Virology*

Role of the C-Terminal Region of Vervet Monkey Polyomavirus 1 VP1 in Virion Formation

Hiroki YAMAGUCHI[1)], Shintaro KOBAYASHI[1)], Junki MARUYAMA[2)], Michihito SASAKI[1)], Ayato TAKADA[2)], Takashi KIMURA[1)], Hirofumi SAWA[1)]* and Yasuko ORBA[1)]

[1)]*Division of Molecular Pathobiology, Research Center for Zoonosis Control, Hokkaido University, Sapporo, Hokkaido 001–0020, Japan*
[2)]*Division of Global Epidemiology, Research Center for Zoonosis Control, Hokkaido University, Sapporo, Hokkaido 001–0020, Japan*

(Received 12 November 2013/Accepted 27 December 2013/Published online in J-STAGE 13 January 2014)

ABSTRACT. Recently, we detected novel vervet monkey polyomavirus 1 (VmPyV) in a vervet monkey. Among amino acid sequences of major capsid protein VP1s of other polyomaviruses, VmPyV VP1 is the longest with additional amino acid residues in the C-terminal region. To examine the role of VmPyV VP1 in virion formation, we generated virus-like particles (VLPs) of VmPyV VP1, because VLP is a useful tool for the investigation of the morphological characters of polyomavirus virions. After the full-length VmPyV VP1 was subcloned into a mammalian expression plasmid, the plasmid was transfected into human embryonic kidney 293T (HEK293T) cells. Thereafter, VmPyV VLPs were purified from the cell lysates of the transfected cells via sucrose gradient sedimentation. Electron microscopic analyses revealed that VmPyV VP1 forms VLPs with a diameter of approximately 50 nm that are exclusively localized in cell nuclei. Furthermore, we generated VLPs consisting of the deletion mutant VmPyV VP1 (ΔC VP1) lacking the C-terminal 116 amino acid residues and compared its VLP formation efficiency and morphology to those of VLPs from wild-type VmPyV VP1 (WT VP1). WT and ΔC VP1 VLPs were similar in size, but the number of ΔC VP1 VLPs was much lower than that of WT VP1 VLPs in VP1-expressing HEK293T cells. These results suggest that the length of VP1 is unrelated to virion morphology; however, the C-terminal region of VmPyV VP1 affects the efficiency of its VLP formation.

KEY WORDS: electron microscopy, polyomavirus, vervet monkey, virus-like particles (VLPs).

doi: 10.1292/jvms.13-0568; *J. Vet. Med. Sci.* 76(5): 637–644, 2014

Polyomaviruses (PyVs), members of the family *Polyomaviridae*, carry a circular double-stranded DNA genome of approximately 5,000 base pairs (bp) in size. PyV genomes consist of three functional regions: an early coding region, a late coding region and a transcriptional control region. The early coding region encodes the regulatory proteins, including small t antigen (tAg) and large T antigen (TAg), which are necessary for viral genome replication and viral gene transcription. The late coding region encodes the structural proteins, such as VP1, VP2 and VP3. In addition, some PyVs also encode agnoprotein in the late coding region. The transcriptional control region contains replication origin and promoter and enhancer sequences and regulates the replication of the viral genome and bidirectional viral transcription for both early and late genes [15, 24].

The virions of PyVs are non-enveloped and icosahedral with a diameter of approximately 45–50 nm and an outer surface consisting mainly of the capsid protein VP1. The PyV capsid is formed by 72 VP1 pentamers, and each of them is arranged in a T=7 icosahedral lattice [13]. Other capsid proteins, VP2 and VP3, extend from the core into the axial cavity of the pentamers.

In the past few years, novel human and non-human primate PyVs have been identified [1, 11, 20, 23]. We also identified a novel PyV, vervet monkey PyV 1 (VmPyV), in a vervet monkey (VM) [27] by using a nested broad-spectrum PCR method [7]. The obtained entire VmPyV genome is 5,157 bp in size and has tAg, TAg, VP1 and VP2 open reading frames (ORFs). VmPyV encodes the unique extended C-terminal VP1 protein of 503 amino acids (a.a.), whereas typical PyVs, such as simian virus 40 (SV40) and JC PyV (JCV), encode VP1s with lengths of 364 and 354 a.a., respectively [19, 21]. VP1s with the long C-terminal regions are also observed in some other PyVs, such as piliocolobus rufomitratus PyV (502 a.a.), chimpanzee PyV (ChPyV, 497 a.a.), california sea lion PyV (495 a.a.), bat PyV (472 a.a.) and merkel cell PyV (423 a.a.) [4–6, 20, 26]. Although it has been reported that the C-terminal tail of VP1 extends out of the pentamer and contacts the neighboring pentamers [9, 13, 22], the function of the long C-terminal region of VP1 is still unclear.

It is known that recombinant PyV VP1s expressed in *Escherichia coli* (*E. coli*), yeast cells, insect cells or mammalian cells are able to self-assemble into virus-like particles (VLPs) without viral genomic DNA and VP2/VP3 [2, 3, 10, 17, 25, 28]. In this study, we generated VmPyV VLPs and examined their morphology by using electron microscopy to determine the role of the C-terminal region of VmPyV VP1 in virion formation.

*CORRESPONDENCE TO: SAWA, H., Division of Molecular Pathobiology, Research Center for Zoonosis Control, Hokkaido University, Kita 20, Nishi 10, Kita-ku, Sapporo, Hokkaido 001–0020, Japan. e-mail: h-sawa@czc.hokudai.ac.jp

©2014 The Japanese Society of Veterinary Science

This is an open-access article distributed under the terms of the Creative Commons Attribution Non-Commercial No Derivatives (by-nc-nd) License <http://creativecommons.org/licenses/by-nc-nd/3.0/>.

MATERIALS AND METHODS

Cells: HEK293T, human embryonic kidney 293 cell line expressing SV40 TAg, cells were maintained under an atmosphere of 5% CO_2 at 37°C in Dulbecco's minimum essential medium supplemented with 10% FBS (fetal bovine serum), 2 mM L-glutamine, penicillin (100 U ml^{-1}) and streptomycin (0.1 mg ml^{-1}). All experiments using HEK293T cells were performed in collagen-coated dishes (Iwaki, Chiba, Japan).

Plasmids and transfection: For expression of VmPyV VP1, the full-length VmPyV VP1 gene was amplified from the VmPyV genomic DNA (GenBank accession number: AB767298) with *Xho*I and *Not*I restriction sites added to the 5′ and 3′ ends, respectively. The PCR product was cloned into the *Xho*I-*Not*I restriction sites of a pCMV-FLAG vector, so that a FLAG tag was added to the N-terminal of expressed VP1. The C-terminal deletion mutant of VmPyV VP1 was also cloned into the vector. These plasmids were transfected into HEK293T cells individually using the Lipofectamine 2000 according to the manufacturer's instructions (Invitrogen, Carlsbad, CA, U.S.A.).

Immunocytochemical and immunoblot analyses: HEK293T cells transfected with the plasmids were collected at 48 hr post transfection. The cells were washed with PBS, fixed in 100% methanol for 5 min at −30°C and blocked with 1% BSA (bovine serum albumin) in PBS containing 0.5% Triton X-100, followed by incubation with an anti-SV40 VP1 antibody overnight at 4°C [8]. The cells were visualized with secondary antibodies (Alexa Fluor 488-conjugated goat anti-rabbit IgG; Invitrogen) and 4′, 6-diamidino-2-phenylindole dihydrochloride (DAPI; Invitrogen) for 1 hr at room temperature. All the fluorescent images were captured and analyzed using a microscope (IX70; Olympus, Tokyo, Japan), a charge-coupled device camera (DP30BW; Olympus) and DP Controller software (Olympus).

For immunoblot analysis, the cells were harvested in RIPA buffer [10 mM Tris-HCl (pH 7.5), 5 mM EDTA, 150 mM NaCl, 10% glycerol, 1% Triton X-100, 1% deoxycholic acid, 0.1% SDS and 50 mM NaF], supplemented with Complete Protease Inhibitor Cocktail (Roche Diagnostics, Indianapolis, IN, U.S.A.) [18]. Cell lysates were centrifuged at 20,400 × *g* for 15 min at 4°C, and the resulting supernatants were subjected to sodium dodecyl sulphate-polyacrylamide gel electrophoresis (SDS-PAGE) and immunoblotting with the following primary antibodies overnight at 4°C; an anti-SV40 VP1 antibody [8] and an anti-actin antibody (MAB1501; Millipore, Bedford, MA, U.S.A.). Actin was used as a loading control. After washing the membrane with TBST (Tris-buffered saline containing 0.05% Tween 20), the membrane was incubated with the following secondary antibodies for 1 hr at room temperature; a horseradish peroxidase (HRP)-conjugated anti-rabbit IgG (Biosource International, Camarillo, CA, U.S.A.) and HRP-conjugated anti-mouse IgG (Biosource International). The immune complexes were detected with Immobilon Western HRP Substrate (Millipore). The chemiluminescence signals were visualized using a VersaDoc 5000MP (Bio-Rad, Hercules, CA, U.S.A.), and images were analyzed using Quantity One software (Bio-Rad).

Electron microscopy: Ultra-thin-section electron microscopy was performed as described previously [16]. In brief, 48 hr post transfection cells were fixed with 2.5% glutaraldehyde in 0.1 M cacodylate buffer (pH 7.3) for 20 min at 4°C. The cells were scraped from the dish and fixed with 2% osmium tetroxide in the same buffer for 1 hr at 4°C. Pellets were dehydrated with a series of ethanol gradients (50%, 70%, 90% and 99.5%) followed by propylene oxide, embedded in Epon 812 Resin mixture (TAAB Laboratories Equipment, Berkshire, U.K.) and polymerized for 3 days at 60°C. Thin-sections (70 nm) were stained with uranyl acetate and lead citrate.

For negative staining, purified fractions fixed with 0.25% glutaraldehyde were adsorbed to collodion-carbon-coated copper grids (Nisshin EM Corporation, Tokyo, Japan) and negatively stained with 2% phosphotungstic acid solution (pH 5.8). All samples were examined with an H-7650 electron microscope at 80 kV (Hitachi, Kyoto, Japan) [14].

Sucrose gradient sedimentation analysis: Sucrose gradient sedimentation analysis was performed as described previously [24]. Briefly, 72 hr post transfection cells were harvested in 10 mM Tris-HCl (pH 7.5), 2 mM $MgCl_2$ and 0.25% Brij 58 (Sigma, St. Louis, MO, U.S.A.). The cellular lysates were subjected to three cycles of freezing and thawing, cellular debris was removed via centrifugation at 500 × *g* for 10 min at 4°C, and the resulting supernatants overlaid onto a preformed 30–50% sucrose gradient in 20 mM Tris-HCl (pH 8.0). Samples were centrifuged at 192,000 × *g* for 1 hr at 4°C (SW55 Ti rotor, Beckman Coulter, Brea, CA, U.S.A.), and each 400 μl fraction was taken from the top for 12 fractions. Each fraction was subjected to SDS-PAGE and immunoblotting with the anti-SV40 VP1 antibody overnight at 4°C [8]. After washing the membrane with TBST, the membrane was incubated with HRP-conjugated anti-rabbit IgG for 1 hr at room temperature (Biosource International). The immune complexes were detected, and the chemiluminescence signals were visualized.

JCV VLPs were prepared as previously described [10]. In brief, BL21 (DE3) pLysS competent cells (Stratagene, La Jolla, CA, U.S.A.) were transformed with the pET15b plasmid (Novagen, Madison, WI, U.S.A.) encoding the full-length JCV VP1 gene, and VLPs were purified.

RESULTS

Expression of VmPyV VP1 in HEK293T cells: The full-length of VmPyV VP1 gene was amplified and cloned into the pCMV-FLAG vector. In addition, we synthesized a C-terminal deletion mutant of VmPyV VP1 (ΔC VP1). The deleted region was determined based on the amino acid sequences alignment with the reported PyV VP1s (Fig. 1). We synthesized the ΔC VP1 of 1–387 amino acid residues of wild-type VmPyV VP1 (WT VP1). The C-terminal deletion mutant VP1 gene with a stop codon (TAA) was also amplified and cloned into the pCMV-FLAG vector. These plasmids were transfected into HEK293T cells individually and incubated for 48 hr. To detect the VP1 protein expression,

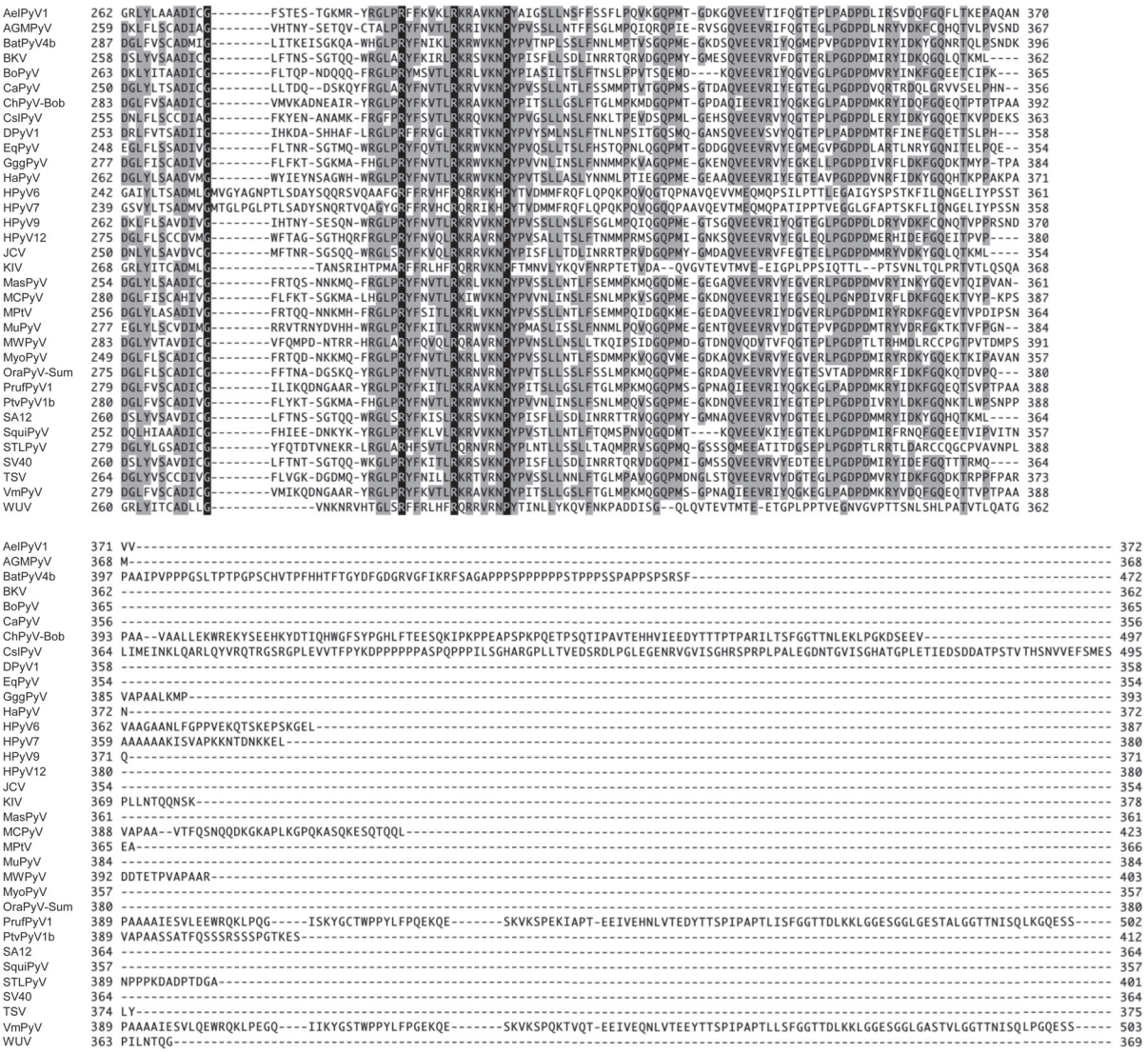

Fig. 1. Alignment of PyV VP1s in C-terminal portions. Alignment of PyV VP1s in C-terminal portions with that of VmPyV. The VP1 sequences of PyVs were obtained from GenBank (abbreviations and accession numbers are indicated in Table 1). Amino acid identities are shaded as follows: black shading indicates that all amino acid sequences were conserved, whereas grey shading indicates that more than 51% of them were conserved.

we performed immunocytochemical analysis using an anti-SV40 VP1 antibody. Intracellular distributions of WT and ΔC VP1s were similar. Both WT and ΔC VP1s were mainly detected in the nuclei and sometimes in the cytoplasm in transfected cells with encoding WT or ΔC VP1 plasmids (Fig. 2A). We also performed immunoblotting analysis to confirm the expression levels of WT and ΔC VP1s. We detected both WT and ΔC VP1s in the cells using the anti-SV40 VP1 antibody at the expected molecular weights of 56 and 44 kDa, respectively (Fig. 2B). Because ΔC VP1 is devoid of 388–503 amino acid residues (116 a.a. deletion), its molecular weight is smaller than that of WT VP1. The expression levels of WT and ΔC VP1s were almost similar relative to the expression levels of internal control protein actin (Fig. 2B). These results suggested that the intracellular localization and expression levels of WT and ΔC VP1s were similar in the transfected cells.

Expression of VLPs using electron microscopy: Because the VmPyV VP1 was detected in transfected HEK293T cells, we confirmed the formation of VLPs using transmission electron microscopy (TEM). At 48 hr post transfection of WT and ΔC VP1 encoding plasmids, scraped cells were embedded in Epon resin and polymerized. Ultra-thin-sections with a thickness of 70 nm were stained with uranyl acetate and lead citrate. TEM revealed a large number of VLPs with a diameter of approximately 50 nm in the nuclei of WT VP1-expressing cells (WT VLPs; Fig. 3A–3C). We were also able to confirm VLPs with a diameter of approxi-

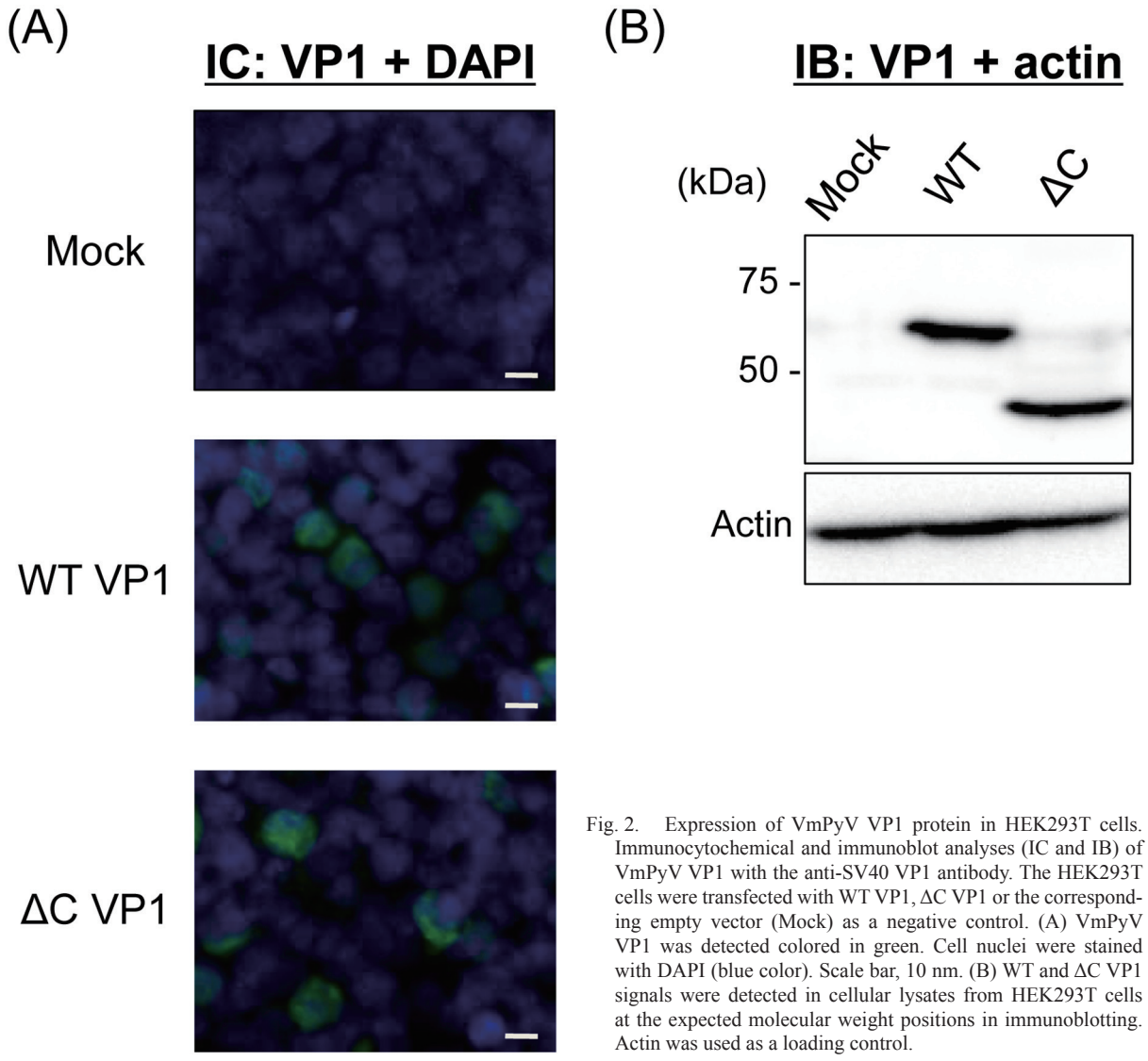

Fig. 2. Expression of VmPyV VP1 protein in HEK293T cells. Immunocytochemical and immunoblot analyses (IC and IB) of VmPyV VP1 with the anti-SV40 VP1 antibody. The HEK293T cells were transfected with WT VP1, ΔC VP1 or the corresponding empty vector (Mock) as a negative control. (A) VmPyV VP1 was detected colored in green. Cell nuclei were stained with DAPI (blue color). Scale bar, 10 nm. (B) WT and ΔC VP1 signals were detected in cellular lysates from HEK293T cells at the expected molecular weight positions in immunoblotting. Actin was used as a loading control.

mately 45–50 nm in the nuclei of ΔC VP1-expressing cells (ΔC VLPs; Fig. 3D–3F); however, the number of ΔC VP1 VLPs was much lower than that of WT VP1 VLPs.

Sucrose gradient sedimentation analysis: To confirm that VLPs were formed by VmPyV VP1 in transfected cells, we also performed the sucrose gradient sedimentation analysis, which can distinguish VLPs from VP1 pentamers [9]. As a positive control in the analysis, we used purified JCV VLPs [10]. After ultracentrifugation, 12 fractions of 400 μl each were dispensed. Each fraction was analyzed by immunoblotting with the anti-SV40 VP1 antibody. The VP1 signal in JCV VLPs was mainly detected in fractions 6 to 9 (Fig. 4A). The VP1 signal in cellular lysates from the WT VP1-expressing cells was also mainly detected in fractions 6 to 9 (Fig. 4B). However, the VP1 signal in cellular lysates from ΔC VP1-expressing cells was mainly detected in fractions 1 to 4 and slightly detected in fractions 5 to 8 (Fig. 4C). To confirm the formation of WT VLPs in fractions 6 to 9, we collected these fractions and verified them with negative-stained TEM. We observed a large number of WT VLPs with a diameter of approximately 50 nm (Fig. 4D). We also confirmed the presence of JCV VLPs in fractions 6 to 9 (data not shown).

DISCUSSION

VmPyV was originally detected in a VM spleen using nested broad-spectrum PCR techniques. It has a longer VP1 ORF in the C-terminus region compared with the sequences of other known PyVs VP1s, whereas its functions are still unclear [27]. In general, the PyV capsid contains 360 molecules of VP1 formed with 72 pentamers, 5 molecules of VP1 and 1 molecule of VP2/VP3 [13, 22]. In the current study, to examine the role of C-terminal of VmPyV VP1 in virion formation, VmPyV VLPs consisting of WT VP1 or ΔC VP1 were generated in mammalian HEK293T cells.

Immunocytochemical analysis revealed that WT and

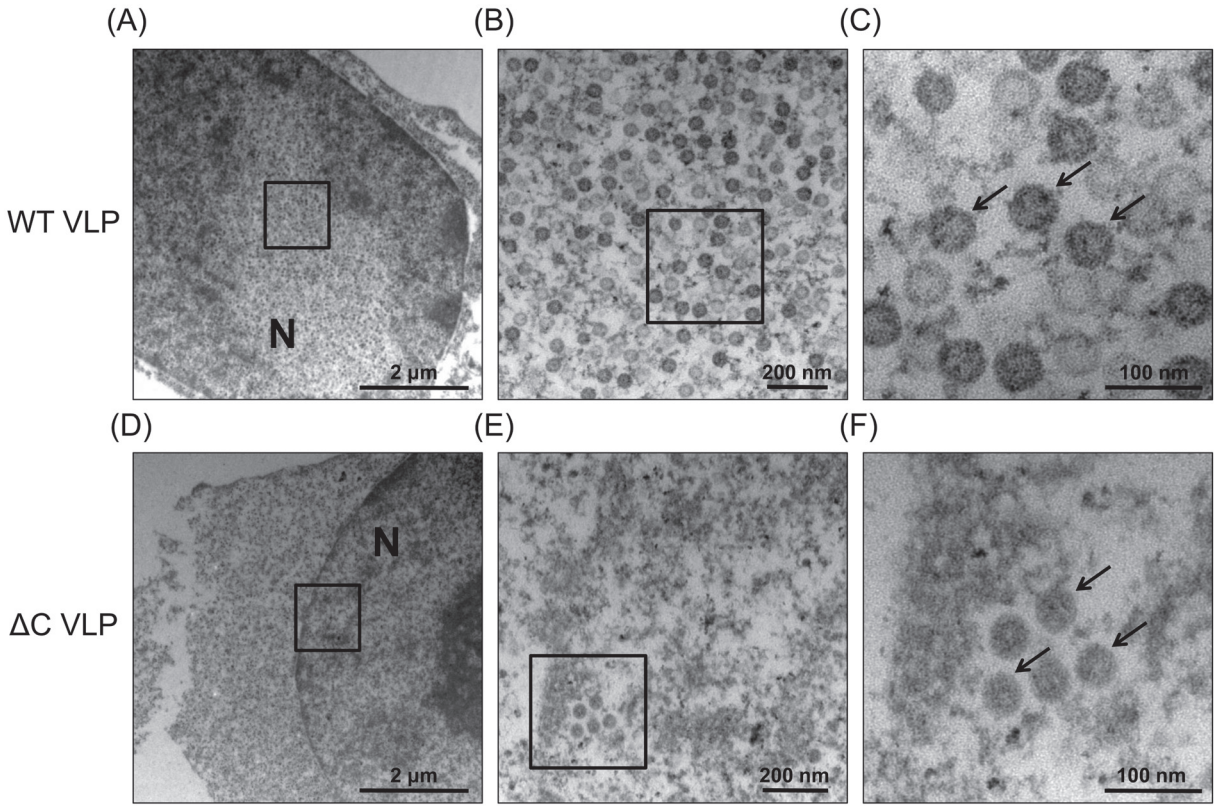

Fig. 3. Electron micrographs of WT VP1 and ΔC VP1-expressing cells. Electron micrographs of HEK293T cells expressing WT VP1 (A–C) and ΔC VP1 (D–F). (B, C, E and F) Higher magnification of the regions indicated in panels A, B, D and E, respectively. All WT and ΔC VLPs were observed exclusively in the nuclei. The arrows indicate VLPs. N: nucleus.

ΔC VP1s were expressed in the transfected HEK293T cells (Fig. 2A). Both WT and ΔC VP1s were also detected at the expected molecular weights by immunoblot analysis (Fig. 2B). Furthermore, there was no difference in the expression level between WT and ΔC VP1s (Fig. 2B). Although VLPs were observed in WT and ΔC VP1-expressing cells by using electron microscopy (Fig. 3), the number of WT VLPs was higher than that of ΔC VLPs. In addition, the number of cells with WT VLPs was higher than that of cells with ΔC VLPs (data not shown). The WT and ΔC VLPs were morphologically indistinguishable. WT and ΔC VLPs were observed in the nuclei; however, no VLPs were confirmed in the cytoplasm (data not shown). We also performed a sucrose gradient sedimentation analysis [9]. Immunoblot analysis revealed that the signal of JCV VLPs was mainly detected in fractions 6 to 9 (Fig. 4A). The VP1 signal in cellular lysates from WT VP1-expressing cells was also mainly detected in fractions 6 to 9 (Fig. 4B). We confirmed the presence of JCV VLPs and WT VLPs in fractions 6 to 9 with negative-stained TEM (Fig. 4D). However, the VP1 signal in cellular lysates from ΔC VP1-expressing cells was mainly detected in fractions 1 to 4 (Fig. 4C). Because the protein density in fractions 1 to 4 is lower than that in fractions 6 to 9, it is supposed that the VP1 signal in fractions 1 to 4 may have represented the pentamers instead of VLPs. In addition, the faint VP1 signal in fractions 5 to 8 of cellular lysates from ΔC VP1-expressing cells may have represented VLPs. This result is convincing in light of the TEM results showing fewer VLPs in ΔC VP1-expressing cells (Fig. 3D–3F). Taken together, the results showed that ΔC VP1 formed VLPs; however, the efficiency of VLP formation was lower than that of WT VP1.

It has been reported that the C-terminal arm of PyVs VP1 can be subdivided into three segments; ‘C helix’, ‘C insert’ and ‘C loop’ [13, 22]. The C helix of SV40 (SFLLSDLINRRTQ; 305–317 a.a.) mediates contacts between pentamers as described previously [13, 22]. As demonstrated in Fig. 1, the C helix of SV40 is predicted to correspond to the 295–307 amino acid residues (SFLLTDLINRRTP) of JCV and the 325–337 amino acid residues (TSLLGSLFTGLMP) of VmPyV. In comparison with tripartite, the homology was 85% for SV40-JCV, 23% for SV40-VmPyV and 31% for JCV-VmPyV in the C helix of VP1s. It revealed that the C-helix of JCV may mediate contacts between pentamers, because of the high homology with that of SV40. However, the C helix of VmPyV has low homology with that of SV40 and JCV. As shown in Fig. 3, we observed that the number of WT VP1 VLPs was much higher than that of ΔC VP1 VLPs. Thus, the deleted C-terminal 116 amino acid residues (388–503 a.a.) of VmPyV VP1 affect the efficiency of its

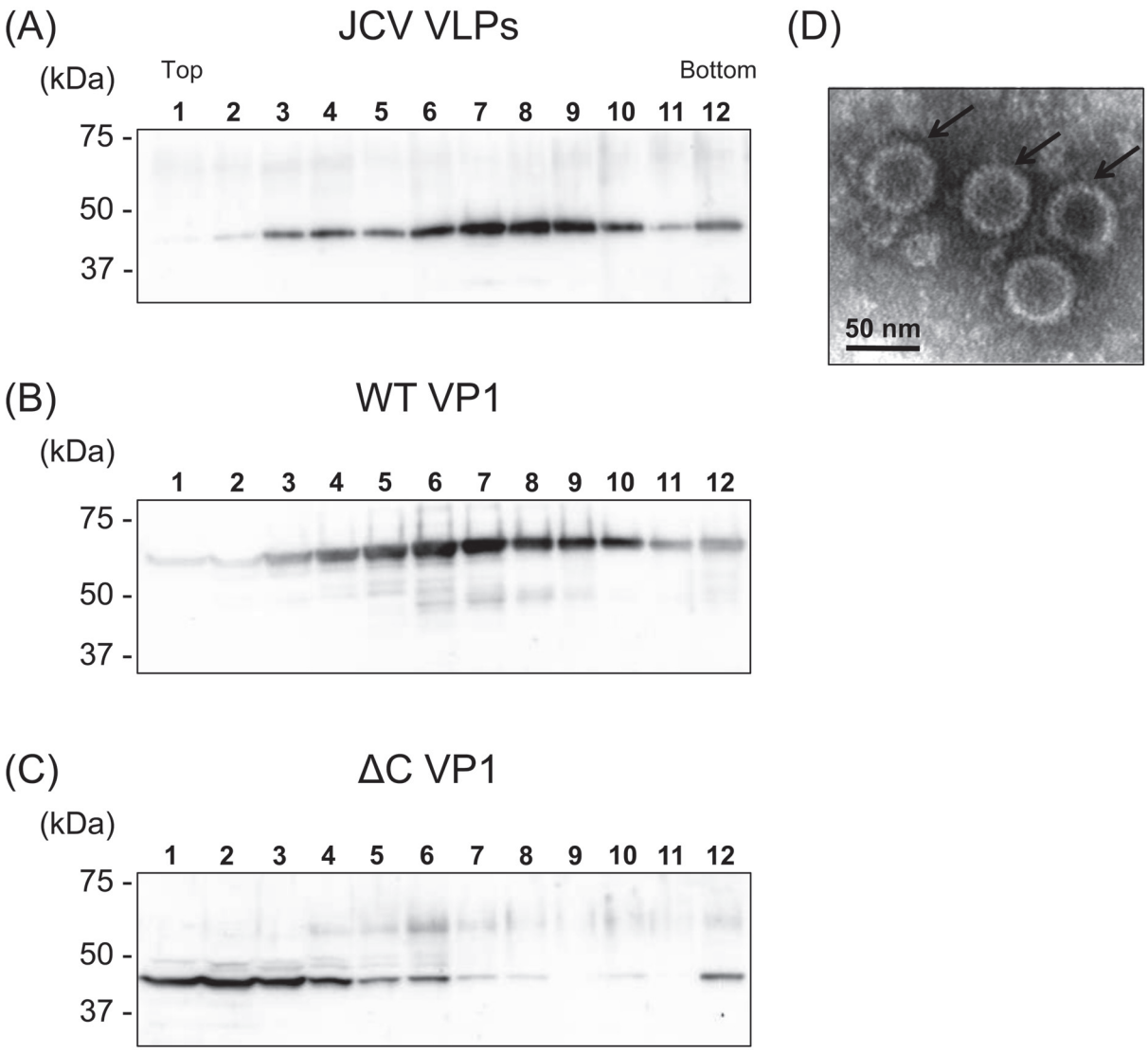

Fig. 4. Sucrose gradient sedimentation analyses. (A–C) Immunoblot analyses of VP1 in fractionated samples after sucrose gradient sedimentation of JCV VLPs and cellular lysates from HEK293T cells expressing WT VP1 or ΔC VP1. Cellular lysates were separated by 30–50% sucrose gradient sedimentation and fractionated into 12 fractions from the tops of the tubes. The 12 fractions were separated by SDS-PAGE and subjected to immunoblotting with the anti-SV40 VP1 antibody. (A) Purified JCV VLPs expressed in *E. coli*. (B) HEK293T cell lysates transfected with WT VP1 and (C) ΔC VP1. (D) Electron micrograph of negative staining of fractions 6 to 9 from HEK293T cells transfected with WT VP1. The arrows indicate VmPyV VLPs

VLP formation.

ChPyV also encodes a unique extended C-terminal VP1 protein of 497 a.a., and ChPyV VLPs were expressed with a diameter of approximately 45 nm [28]. The diameter of VmPyV WT VLPs is approximately 50 nm (Fig. 4D). These results suggest that the length of VP1 amino acid residues has no effect on the size (i.e., diameter) of VLPs. It has been reported that SV40 VLPs made exclusively of VP1 and native SV40 virions were morphologically indistinguishable under electron microscopy [12]. We observed that VmPyV VLPs have a typical shape of PyV virions, and their diameters were approximately 50 nm in size, suggesting that native VmPyV virions also have morphology similar to that of its VLPs.

In conclusion, we demonstrated that VmPyV VLPs were formed in mammalian cells expressing VP1 and found the extra C-terminal region of VP1 does not affect the size and morphology of VLPs, whereas the C-terminal of VmPyV VP1 may have some function for efficient VLP formation. The study to investigate function (s) of the extra C-terminal region of VmPyV VP1 needs to be continued.

ACKNOWLEDGMENTS. We thank Dr. Osamu Ichii (Laboratory of Anatomy, Graduate Veterinary Medicine, Hokkaido

Table 1. Abbreviations and accession numbers of VP1 protein sequences of referenced PyVs

Polyomaviruses (PyVs)	Abbreviations	Accession numbers of VP1
African elephant PyV 1	AelPyV1	AGV77094
African green monkey PyV	AGMPyV	NP_848007
Bat PyV 4b (C1109)	BatPyV4b	AFP94194
BK PyV	BKV	CAA24299
Bovine PyV	BoPyV	NP_040787
Canary PyV	CaPyV	ADM88650
Chimpanzee PyV (Bob)	ChPyV-Bob	CBX23438
California sea lion PyV	CslPyV	ADC34409
Dolphin PyV 1	DPyV1	AGR44739
Equine PyV	EqPyV	YP_006383691
Gorilla gorilla gorilla PyV	GggPyV	ADQ54207
Hamster PyV	HaPyV	AAA67119
Human PyV 6	HPyV6	YP_003848918
Human PyV 7	HPyV7	YP_003848923
Human PyV 9	HPyV9	YP_004243705
Human PyV 12	HPyV12	AFP94186
JC PyV	JCV	AAA82101
KI PyV	KIV	ABN09917
Mastomys PyV	MasPyV	BAJ53086
Merkel Cell PyV	MCPyV	YP_001651048
Murine pneumotropic virus	MPtV	ABM67407
Murine PyV	MuPyV	AAA46875
MW PyV	MWPyV	AFN02454
Myotis PyV	MyoPyV	YP_002261488
Orangutan PyV (Sumatra)	OraPyV-Sum	CAX87757
Piliocolobus rufomitratus PyV 1	PrufPyV1	AFU25596
Pan troglodytes verus PyV 1b (6520)	PtvPyV1b	ADQ54182
Simian agent 12	SA12	AAV75982
Squirrel monkey PyV	SquiPyV	YP_001531348
STL PyV	STLPyV	AGC03169
Simian virus 40	SV40	AAB59923
Trichodysplasia spinulosa-associated PyV	TSV	YP_003800006
Vervet monkey PyV 1	VmPyV	BAM71868
WU PyV	WUV	ABQ09289

University, Sapporo, Japan) for assistance with thin-section staining and Dr. Harumi Kasamatsu (Department of Molecular, Cell and Developmental Biology and Molecular Biology Institute, University of California at Los Angeles, Los Angeles, CA) for providing the polyclonal anti-SV40 VP1 antibody. This study was supported in part by grants from the Ministry of Education, Culture, Sports, Science and Technology (MEXT), JST KAKENHI Grant Number 24405043; the Ministry of Health, Labour and Welfare of Japan; and the Japan Initiative for Global Research Network on Infectious Diseases (J-GRID), as well as by the Grant from the Ministry of Education, Culture, Sports, Science and Technology, Japan, for Joint Research Program of the Research Center for Zoonosis Control, Hokkaido University.

REFERENCES

1. Anthony, S. J., St Leger, J. A., Navarrete-Macias, I., Nilson, E., Sanchez-Leon, M., Liang, E., Seimon, T., Jain, K., Karesh, W., Daszak, P., Briese, T. and Lipkin, W. I. 2013. Identification of a novel cetacean polyomavirus from a common dolphin (Delphinus delphis) with Tracheobronchitis. *PLoS ONE* **8**: e68239. [Medline] [CrossRef]
2. Chang, D., Fung, C. Y., Ou, W. C., Chao, P. C., Li, S. Y., Wang, M., Huang, Y. L., Tzeng, T. Y. and Tsai, R. T. 1997. Self-assembly of the JC virus major capsid protein, VP1, expressed in insect cells. *J. Gen. Virol.* **78**: 1435–1439. [Medline]
3. Chen, P. L., Wang, M., Ou, W. C., Lii, C. K., Chen, L. S. and Chang, D. 2001. Disulfide bonds stabilize JC virus capsid-like structure by protecting calcium ions from chelation. *FEBS Lett.* **500**: 109–113. [Medline] [CrossRef]
4. Deuzing, I., Fagrouch, Z., Groenewoud, M. J., Niphuis, H., Kondova, I., Bogers, W. and Verschoor, E. J. 2010. Detection and characterization of two chimpanzee polyomavirus genotypes from different subspecies. *Virol. J.* **7**: 347. [Medline] [CrossRef]
5. Fagrouch, Z., Sarwari, R., Lavergne, A., Delaval, M., de Thoisy, B., Lacoste, V. and Verschoor, E. J. 2012. Novel polyomaviruses in South American bats and their relationship to other members of the Polyomaviridae. *J. Gen. Virol.* **93**: 2652–2657. [Medline]

[CrossRef]
6. Feng, H., Shuda, M., Chang, Y. and Moore, P. S. 2008. Clonal integration of a polyomavirus in human Merkel cell carcinoma. *Science* **319**: 1096–1100. [Medline] [CrossRef]
7. Johne, R., Enderlein, D., Nieper, H. and Müller, H. 2005. Intracellular localization of viral polypeptides during simian virus 40 infection. *J. Virol.* **32**: 648–660.
8. Kasamatsu, H. and Nehorayan, A. 1979. Intracellular localization of viral polypeptides during simian virus 40 infection. *J. Virol.* **32**: 648–660. [Medline]
9. Kawano, M. A., Inoue, T., Tsukamoto, H., Takaya, T., Enomoto, T., Takahashi, R. U., Yokoyama, N., Yamamoto, N., Nakanishi, A., Imai, T., Wada, T., Kataoka, K. and Handa, H. 2006. The VP2/VP3 minor capsid protein of simian virus 40 promotes the in vitro assembly of the major capsid protein VP1 into particles. *J. Biol. Chem.* **281**: 10164–10173. [Medline] [CrossRef]
10. Kobayashi, S., Suzuki, T., Igarashi, M., Orba, Y., Ohtake, N., Nagakawa, K., Niikura, K., Kimura, T., Kasamatsu, H. and Sawa, H. 2013. Cysteine Residues in the Major Capsid Protein, Vp1, of the JC Virus Are Important for Protein Stability and Oligomer Formation. *PLoS ONE* **8**: e76668. [Medline] [CrossRef]
11. Korup, S., Rietscher, J., Calvignac-Spencer, S., Trusch, F., Hofmann, J., Moens, U., Sauer, I., Voigt, S., Schmuck, R. and Ehlers, B. 2013. Identification of a novel human polyomavirus in organs of the gastrointestinal tract. *PLoS ONE* **8**: e58021. [Medline] [CrossRef]
12. Kosukegawa, A., Arisaka, F., Takayama, M., Yajima, H., Kaidow, A. and Handa, H. 1996. Purification and characterization of virus-like particles and pentamers produced by the expression of SV40 capsid proteins in insect cells. *Biochim. Biophys. Acta.* **1290**: 37–45. [Medline] [CrossRef]
13. Liddington, R. C., Yan, Y., Moulai, J., Sahli, R., Benjamin, T. L. and Harrison, S. C. 1991. Structure of simian virus 40 at 3.8-A resolution. *Nature* **354**: 278–284. [Medline] [CrossRef]
14. Maruyama, J., Miyamoto, H., Kajihara, M., Ogawa, H., Maeda, K., Sakoda, Y., Yoshida, R. and Takada, A. 2014. Characterization of the envelope glycoprotein of a novel filovirus, Lloviu virus. *J. Virol.* **88**: 99–109. [Medline] [CrossRef]
15. Moens, U., Van Ghelue, M., Song, X. and Ehlers, B. 2013. Serological cross-reactivity between human polyomaviruses. *Rev. Med. Virol.* **23**: 250–264. [Medline] [CrossRef]
16. Noda, T., Sagara, H., Suzuki, E., Takada, A., Kida, H. and Kawaoka, Y. 2002. Ebola virus VP40 drives the formation of virus-like filamentous particles along with GP. *J. Virol.* **76**: 4855–4865. [Medline] [CrossRef]
17. Ou, W. C., Wang, M., Fung, C. Y., Tsai, R. T., Chao, P. C., Hseu, T. H. and Chang, D. 1999. The major capsid protein, VP1, of human JC virus expressed in Escherichia coli is able to self-assemble into a capsid-like particle and deliver exogenous DNA into human kidney cells. *J. Gen. Virol.* **80**: 39–46. [Medline]
18. Orba, Y., Kobayashi, S., Nakamura, I., Ishii, A., Hang'ombe, B. M., Mweene, A. S., Thomas, Y., Kimura, T. and Sawa, H. 2011. Detection and characterization of a novel polyomavirus in wild rodents. *J. Gen. Virol.* **92**: 789–795. [Medline] [CrossRef]
19. Padgett, B. L., Zurhein, G. M., Walker, D. L., Eckroade, R. J. and Dessel, B. H. 1971. Cultivation of papova-like virus from human brain with progressive multifocal leucoencephalopathy. *Lancet* **297**: 1257–1260. [Medline] [CrossRef]
20. Scuda, N., Madinda, N. F., Akoua-Koffi, C., Adjogoua, E. V., Wevers, D., Hofmann, J., Cameron, K. N., Leendertz, S. A., Couacy-Hymann, E., Robbins, M., Boesch, C., Jarvis, M. A., Moens, U., Mugisha, L., Calvignac-Spencer, S., Leendertz, F. H. and Ehlers, B. 2013. Novel polyomaviruses of nonhuman primates: genetic and serological predictors for the existence of multiple unknown polyomaviruses within the human population. *PLoS Pathog.* **9**: e1003429. [Medline] [CrossRef]
21. Shah, K. and Nathanson, N. 1976. Human exposure to SV40: review and comment. *Am. J. Epidemiol.* **103**: 1–12. [Medline]
22. Stehle, T., Gamblin, S. J., Yan, Y. and Harrison, S. C. 1996. The structure of simian virus 40 refined at 3.1 A resolution. *Structure* **4**: 165–182. [Medline] [CrossRef]
23. Stevens, H., Bertelsen, M. F., Sijmons, S., Van Ranst, M. and Maes, P. 2013. Characterization of a Novel Polyomavirus Isolated from a Fibroma on the Trunk of an African Elephant (Loxodonta africana). *PLoS ONE* **8**: e77884. [Medline] [CrossRef]
24. Suzuki, T., Semba, S., Sunden, Y., Orba, Y., Kobayashi, S., Nagashima, K., Kimura, T., Hasegawa, H. and Sawa, H. 2012. Role of JC virus agnoprotein in virion formation. *Microbiol. Immunol.* **56**: 639–646. [Medline] [CrossRef]
25. Tolstov, Y. L., Pastrana, D. V., Feng, H., Becker, J. C., Jenkins, F. J., Moschos, S., Chang, Y., Buck, C. B. and Moore, P. S. 2009. Human Merkel cell polyomavirus infection II. MCV is a common human infection that can be detected by conformational capsid epitope immunoassays. *Int. J. Cancer* **125**: 1250–1256. [Medline] [CrossRef]
26. Wellehan, J. F., Rivera, R., Archer, L. L., Benham, C., Muller, J. K., Colegrove, K. M., Gulland, F. M., St Leger, J. A., Venn-Watson, S. K. and Nollens, H. H. 2011. Characterization of California sea lion polyomavirus 1: expansion of the known host range of the Polyomaviridae to Carnivora. *Infect. Genet. Evol.* **11**: 987–996. [Medline] [CrossRef]
27. Yamaguchi, H., Kobayashi, S., Ishii, A., Ogawa, H., Nakamura, I., Moonga, L., Hang'ombe, B. M., Mweene, A. S., Thomas, Y., Kimura, T., Sawa, H. and Orba, Y. 2013. Identification of a novel polyomavirus from vervet monkeys in Zambia. *J. Gen. Virol.* **94**: 1357–1364. [Medline] [CrossRef]
28. Zielonka, A., Verschoor, E. J., Gedvilaite, A., Roesler, U., Müller, H. and Johne, R. 2011. Detection of chimpanzee polyomavirus-specific antibodies in captive and wild-caught chimpanzees using yeast-expressed virus-like particles. *Virus Res.* **155**: 514–519. [Medline] [CrossRef]